JACS
JOURNAL OF THE AMERICAN CHEMICAL SOCIETY

Subscriber access provided by American Chemical Society

Article

Pathways for Photoinduced Charge Separation in DNA Hairpins

D. Beljonne, G. Pourtois, M. A. Ratner, and J. L. Brdas

J. Am. Chem. Soc., **2003**, 125 (47), 14510-14517• DOI: 10.1021/ja035596f • Publication Date (Web): 30 October 2003

Downloaded from http://pubs.acs.org on March 30, 2009

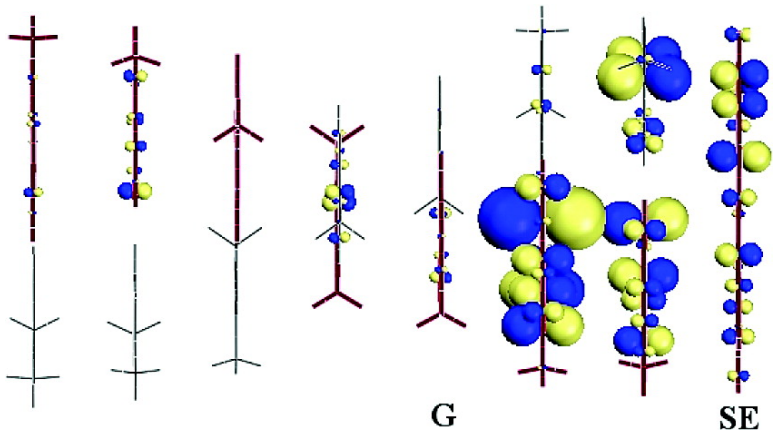

More About This Article

Additional resources and features associated with this article are available within the HTML version:

- Supporting Information
- Links to the 7 articles that cite this article, as of the time of this article download
- Access to high resolution figures
- Links to articles and content related to this article
- Copyright permission to reproduce figures and/or text from this article

View the Full Text HTML

ACS Publications
High quality. High impact.

Journal of the American Chemical Society is published by the American Chemical Society. 1155 Sixteenth Street N.W., Washington, DC 20036

J|A|C|S
ARTICLES
Published on Web 10/30/2003

Pathways for Photoinduced Charge Separation in DNA Hairpins

D. Beljonne,[†,‡] G. Pourtois,[†] M. A. Ratner,[§] and J. L. Brédas*[,‡]

Contribution from the Laboratory of Chemistry of Novel Materials, University of Mons-Hainaut, Place du Parc 20, 7000 Mons, Belgium, School of Chemistry and Biochemistry, Georgia Institute of Technology, Atlanta, Georgia 30332-0400, and Department of Chemistry and Materials Research Center, Northwestern University, 2145 North Sheridan Road, Evanston, Illinois 60208

Received April 11, 2003; E-mail: jean-luc.bredas@chemistry.gatech.edu

Abstract: By means of correlated quantum-chemical calculations, we explore the chain-length dependence of the electronic coupling for photoinduced charge separation in DNA hairpins associated to conjugated linkers. Pathways for charge transfer from the linker chromophore to a guanine site located at a well-defined distance along the DNA strand are identified. Importantly, these involve not only the frontier molecular orbitals of the interacting donor, bridge, and acceptor units, but also deeper lying orbitals possessing both the appropriate energy and the symmetry to overlap significantly. The relative efficiency of these channels is found to be sensitive to the chemical structure of the linker, leading to falloff parameters for the charge-transfer rates ranging from ~0.4 to ~1.2 Å^{-1}.

I. Introduction

That DNA can transport charge over large distances is now well established, although questions regarding the mechanisms of the process remain.[1] There is general agreement that a plausible scenario for hole transport in DNA involves superexchange or tunneling at short distances and multistep hopping at long range.[2−6] Such a hopping process involves positive charges moving between guanines (G), which show the lowest ionization potential among the DNA bases (although for large distances between the guanines, hopping of charges between adenine bases becomes operative).[7] Although such a mechanism in principle allows for long-range charge migration, its efficiency is directly controlled by the transfer rate for the individual hopping steps. These are usually predicted to occur by superexchange from the donor (initial site) to a particular acceptor and, therefore, should lead to a fast, exponential decay of the rate, k_{DA}, with donor−acceptor separation, d_{DA}:

$$k_{DA} \propto \exp(-\beta d_{DA}) \quad (1)$$

with β as a characteristic parameter for the bridge conductance: $\beta > 1$ Å^{-1} in insulators such as most proteins[8] and ~0.2 Å^{-1} for a coherent molecular wire.[9] The magnitude of β for the various possible superexchange partners in DNA is still controversial.

An important issue that has not been fully resolved yet is the amount of charge delocalization over neighboring base pairs;[10−15] to put it simply, the more extended the wave function, the better the conductance (in the limiting case of complete charge delocalization, the electron transfer occurs with virtually no distance dependence). The relative localization/delocalization of the charge carriers along the DNA helix is partly controlled by the interplay between the geometric relaxation and medium polarization energies involved with charging the isolated bases, λ, and the interbase electronic couplings, V_{DA}. For $V_{DA}^2/(|E_D - E_A|) \gg \lambda$ (where E_D and E_A are the donor and acceptor site energies, respectively), charges substantially delocalize.[10]

[†] University of Mons-Hainaut.
[‡] Georgia Institute of Technology.
[§] Northwestern University.

(1) Murphy, C. J.; Arkin, M. R.; Jenkins, Y.; Ghatlia, N. D.; Bossmann, S. H.; Turro, N. J.; Barton, J. K. *Science* **1993**, *262*, 1025. Murphy, C. J.; Arkin, M. R.; Ghatlia, N. D.; Bossmann, S.; Turro, N. J.; Barton, J. K. *Proc. Natl. Acad. Sci. U.S.A.* **1994**, *91*, 5315. Diederichsen, U. *Angew. Chem., Int. Ed. Engl.* **1997**, *36*, 2317. Wilson, E. K. *Chem. Eng. News* **1998**, *76*, 51. Wilson, E. K. *Chem. Eng. News* **1999**, *77*, 43. Ratner, M. *Nature* **1999**, *397*, 480. Grinstaff, M. W. *Angew. Chem., Int. Ed.* **1999**, *38*, 3629.
(2) Gasper, S. M.; Schuster, G. B. *J. Am. Chem. Soc.* **1997**, *119*, 12762.
(3) Jortner, J.; Bixon, M.; Langenbacher, T.; Michel-Beyerle, M. E. *Proc. Natl. Acad. Sci. U.S.A.* **1998**, *95*, 12759. Bixon, M.; Jortner, J. *J. Phys. Chem. A* **2001**, *105*, 10322. Bixon, M.; Jortner J. *J. Am. Chem. Soc.* **2001**, *123*, 12556.
(4) Meggers, E.; Michel-Beyerle, M. E.; Giese, B. *J. Am. Chem. Soc.* **1998**, *120*, 12950. Giese, B. *Acc. Chem. Res.* **2000**, *33*, 631.
(5) Berlin, Y. A.; Burin, A. L.; Ratner, M. A. *J. Am. Chem. Soc.* **2001**, *123*, 260.
(6) Smith, D. M. A.; Adamowicz, L. *J. Phys. Chem. B* **2001**, *105*, 9345.
(7) Giese, B.; Amaudrut, J.; Köhler, A. K.; Spormann, M.; Wessely, S. *Nature* **2001**, *412*, 318.
(8) Langen, R.; Chang, I.-J.; Germanas, J. P.; Richards, J. H.; Winkler, J. R.; Gray, H. B. *Science* **1995**, *268*, 1733.
(9) Bixon, M.; Jortner, M. *Adv. Chem. Phys.* **1999**, *106*, 35.
(10) Olofsson, J.; Larsson, S. *J. Phys. Chem. B* **2001**, *105*, 10398.
(11) (a) Conwell, E. M.; Rakhmanova, S. V. *Proc. Natl. Acad. Sci. U.S.A.* **2000**, *97*, 4556. (b) Rakhamanova, S.; Conwell, E. M. *J. Phys. Chem. B* **2001**, *105*, 2056. (c) Conwell, E. M.; Basko, D. M. *J. Am. Chem. Soc.* **2001**, *123*, 11441. (d) Basko, D. M.; Conwell, E. M. *Phys. Rev. Lett.* **2002**, *88*, 098102-1.
(12) Schuster, G. B. *Acc. Chem. Res.* **2000**, *33*, 253.
(13) Kurnikov, I. V.; Tong, G. S. M.; Madrid, M.; Beratan, D. N. *J. Phys. Chem. B* **2002**, *106*, 7.
(14) Barnett, R. N.; Cleveland, C. L.; Joy, A.; Landman, U.; Schuster, G. B. *Science* **2001**, *294*, 567.
(15) Troisi, A.; Orlandi, G. *J. Phys. Chem. B* **2002**, *106*, 2093.

10.1021/ja035596f CCC: $25.00 **© 2003 American Chemical Society**

Tight-binding calculations by Conwell and co-workers indicate that positive and negative charges in DNA can form stable polarons extending over 5−7 base pairs.[11a−c] Similarly, a phonon-assisted polaron hopping model has been proposed by Schuster to explain the long-range charge migration in DNA.[12]

When medium effects are accounted for, Basko and Conwell found that a hole-polaron, in a DNA stack consisting of a single base pair repeated, spreads over 3−5 sites.[11d] On the other hand, based on Hartree−Fock electronic-structure calculations, Kurnikov et al. calculated that the hole self-localizes over a rather compact domain, ∼1 to 3 base pairs.[13] First-principles quantum-mechanical simulations by Barnett et al. have also highlighted the importance of the environment (sugar−phosphate backbone, counterions, and solvating water) on the mechanism of hole transfer in DNA; according to these authors, the hole migration is gated by the configurational dynamics of the counterions, which fixes the amount of charge delocalization along the DNA strands.[14] Troisi and Orlandi have demonstrated that the electronic couplings, V_{DA}, are strongly affected by solvent fluctuations and molecular vibrations;[15] as a consequence, the commonly adopted Franck−Condon approximation with factorization of the charge-transfer rates into electronic and vibrational factors might become inappropriate.[15]

Thus, the effectiveness of the path formed by the stacked DNA base pairs as a channel for charge transport appears to depend on a large number of interconnected factors. These include sequence,[16] conformation and structural disorder along the helix,[17] tradeoff between interbase electronic couplings and intrabase geometric reorganization energy,[10−12] and medium effects.[11d,13−15]

An elegant approach to assess the individual hopping steps in the mechanism for electron transport in DNA has been developed by Lewis et al., who have measured the distance dependence of the charge-transfer rate in synthetic DNA hairpins end-capped with different conjugated linker chromophores.[18] In these experiments, photoexcitation of the hairpin-linker chromophore (hole donor) is followed by migration of the hole to a guanine site (hole acceptor) through intervening AT base pairs. Grozema et al. have proposed a simple phenomenological model based on the tight-binding approximation that relates the magnitude of β in eq 1 to the energy mismatch between the donor and bridge HOMO levels (injection energy) and gives some clue as to the origin of the widespread β values reported in the literature.[19] Ab initio calculations of the interbase electronic couplings by Voityuk et al. have also provided useful insight in this regard.[20] However, these calculations were all based on a one-electron picture, with the electronic tunneling matrix element (for hole migration), V_{DA}, estimated as the energy difference between the HOMO and HOMO−1 energy levels of stacked nucleobase pairs.

Here, we address at the correlated level the dependence with bridge length of the electronic transfer matrix elements for charge injection into DNA, by taking the synthetic hairpins of Lewis et al.[18] as examples. Our goal is two-fold: (i) to provide a simple framework for understanding the relationship between the electronic structure of the hairpins and the distance-dependent photoinduced charge-transfer electronic couplings; and (ii) to unravel the various channels contributing to the charge-transfer process. For this purpose, the initial and final states in the charge-separation process are described by a multiconfigurational (CI, configuration interaction) approach wherein the various paths for charge motion are naturally built in the wave function expansions. We show that including these channels is critical for a proper description of the photoinduced hole-transfer mechanism in DNA.

II. Methodology

The generalized Mulliken−Hush (GMH) formalism has been used to compute the electronic coupling for photoexcited hole transfer (H matrix element between the diabatic states):[21]

$$V_{DA} = \langle \Psi^{diab}_{D^*A} | H | \Psi^{diab}_{D^-A^+} \rangle = \frac{\mu_{RP} \Delta E_{RP}}{\sqrt{(\Delta\mu_{RP})^2 + 4(\mu_{RP})^2}} \quad (2)$$

This expression involves the energy difference (ΔE_{RP}), as well as the corresponding dipole moment difference ($\Delta\mu_{RP}$) and transition dipole moment (μ_{RP}), between the initial (reactant R) and final (product P) electronic adiabatic states. Note that the adiabatic states involved in the process studied here are the lowest optically allowed excited state of the chromophore (D*A) and the charge-transfer state (D^-A^+) resulting from the migration of a hole from the chromophore (hole donor) to the guanine (hole acceptor) along the DNA hairpin. We have computed these parameters by means of the semiempirical Hartree−Fock INDO (intermediate neglect of differential overlap)[22] Hamiltonian coupled to a configuration interaction scheme involving single excitations (SCI) with respect to the Hartree−Fock determinant (the Mataga−Nishimoto[23] potential has been adopted to describe electron−electron interactions). The size of the active space was increased until complete convergence of the transition energies from the ground state to the lowest excited states is achieved. We note that the INDO/SCI calculations are performed in the nuclear arrangement representative of the initial state and that the geometry of this initial state (see below) takes into account the relaxed excited-state geometry of the isolated chromophore (evaluating the relaxed geometry of the chromophore excited state embedded in the full hairpin remains a very difficult task); this approximation is expected to hold for the generally weak donor−acceptor interactions found here but to work less well when the chromophore and the G−C base pair are in close contact.

The use of a many-electron picture allows us to include at once the contributions from all possible pathways for the photoinduced charge transfer. Indeed, within a configuration interaction formalism, the wave functions for the initial (D*A) and final (D^-A^+) excited states can be expanded to first approximation as:

(16) Williams, T. T.; Odom, D. T.; Barton, J. K. *J. Am. Chem. Soc.* **2000**, *122*, 9048.
(17) Hjort, M.; Stafström, S. *Phys. Rev. Lett.* **2001**, *87*, 228101-1-4.
(18) Lewis, F. D.; Wu, T.; Zhang, Y.; Letsinger, R. L.; Greenfield, S. R.; Wasielewski, M. R. *Science* **1997**, *277*, 673. Lewis, F. D.; Wu, T.; Liu, X.; Letsinger, R. L.; Greenfield, S. R.; Miller, S. E.; Wasielewski, M. R. *J. Am. Chem. Soc.* **2000**, *122*, 2889. Lewis, F. D.; Letsinger, R. L.; Wasielewski, M. R. *Acc. Chem. Res.* **2001**, *34*, 159.
(19) Grozema, F. C.; Berlin, Y. A.; Siebbeles, L. D. A. *J. Am. Chem. Soc.* **2000**, *122*, 10903.
(20) Voityuk, A. A.; Rösch, N.; Bixon, M.; Jortner, J. *J. Phys. Chem. B* **2000**, *104*, 9740. Voityuk, A. A.; Jortner, J.; Bixon, M.; Rösch, N. *J. Chem. Phys.* **2001**, *114*, 5614. Voityuk, A. A.; Rösch, N. *J. Phys. Chem. B* **2002**, *106*, 3013.
(21) Cave, J. C.; Newton, M. D. *Chem. Phys. Lett.* **1996**, *249*, 15.
(22) Ridley, J.; Zerner, M. C. *Theor. Chim. Acta* **1973**, *32*, 111.
(23) Mataga, N.; Nishimoto, K. *Z. Phys. Chem.* **1957**, *13*, 140.

$$|\Psi(D^*A)\rangle \approx \sum_i c_i|O_D \rightarrow U_D\rangle \quad \text{and}$$

$$|\Psi(D^-A^+)\rangle \approx \sum_j c_j|O_A \rightarrow U_D\rangle \quad (3)$$

where O_D [U_A] denotes an occupied [unoccupied] molecular orbital mostly localized on the donor [acceptor] and the sum is run over all molecular orbitals included in the CI active space (note that in eq 3, for the sake of simplicity of the discussion, contributions from charge-transfer excitations to D*A and localized donor or acceptor excitations to D^-A^+ are neglected; these contributions are fully taken into account in the actual calculations). The dipole matrix element μ_{RP} involved in the GMH calculation of the electronic coupling between states D*A and D^-A^+, eq 2, can then be recast in an MO representation as

$$\mu_{RP} = \langle\Psi(D^*A)|\hat{\mu}|\Psi(D^-A^+)\rangle = -\sum_{i,j} c_i c_j \langle O_D|\hat{\mu}|O_A\rangle \quad (4)$$

The matrix elements in eq 4 provide a direct measure of the donor−acceptor molecular orbital overlap. Configurations contributing the most to the overall transition moment are hence those leading to the maximum overlap between the involved molecular orbitals (weighted by the expansion coefficients of these configurations to the state descriptions, i.e., c_i and c_j). These correspond to the relevant channels for the hole-transfer process.

The oligonucleotides are modeled as perfect stacks of nucleic acids in which methyl groups substitute for the nucleoside backbones (a distance of 3.4 Å and a rotation angle of 36° are imposed between each base pair). The geometries of the nucleic acids are obtained on the basis of the AMBER molecular mechanics force field,[24] known for providing reliable DNA and protein structures. The excited-state equilibrium geometries of the chromophores have been optimized by combining the AM1 (Austin Model 1)[25] approach to a complete active space configuration interaction (CAS-CI) treatment (as developed in the AMPAC package);[26] the size of the active space in the AM1/CAS-CI calculations has been modulated to ensure convergence of the total energies and geometric parameters. The chromophore/DNA hairpin is then built from the relaxed geometries of the isolated chromophores, assuming a chromophore−base stacking distance of 3.2 Å and a rotation angle of 10°.[27]

We note that part of the environment effects are accounted for in our approach, because the INDO/SCI electronic-structure calculations have been performed for the whole stacks of base pairs (albeit without the sugar and phosphate groups). Thus, polarization effects due to electrostatic interactions between adjacent nucleobases are included through diagonalization of the full Hamiltonian, in contrast to pairwise interaction calculations.[20] These effects, which are very sensitive to the DNA sequences, are found to impact strongly the relative energetic positions of the base molecular orbitals (and, hence, the amount of wave function delocalization from the donor to the acceptor across the DNA bridge) and the magnitude of V_{DA}. As an illustration, it is interesting to realize that the INDO-calculated shift in ionization potential (within Koopmans approximation) when going from an isolated G−C pair to a triplet of adjacent such pairs amounts to 0.76 eV; when the G−C pair(s) is sandwiched between six A−T pairs on each side, the corresponding shift is only 0.14 eV. This difference comes from the intermolecular interactions between the guanine site(s) and the surrounding A−T bases. It is also worth noting that the 0.76 eV INDO shift in ionization potential calculated for isolated GGG versus G sequences is in excellent agreement with the theoretical ab initio 6-31G* value of Sugiyama and Saito (~0.7 eV);[28] the corresponding 0.14 eV ionization potential difference in extended stacks is close to the value (~0.1 eV) calculated by Conwell and Basko[11c] using a tight-binding model in long sequences, including either G or GGG and consistent with the fact that GGG sequences act as shallow hole traps.

To gain some insight into the origin of the different pathways for charge transfer in the DNA hairpins, we used graphical representations in which molecular orbital localization/delocalization, energies, and base spatial distribution are blended. In such plots, each molecular orbital ϕ_i is depicted on the basis of one or several horizontal lines, whose length per base is proportional to the site (r) electron population ($\rho_i(r)$). Within the ZDO formalism, the electron population of a molecular orbital, ϕ_i, on a site r, is computed by summing the squares of the LCAO coefficients ($C_{i\lambda}$) localized on this site:

$$\rho_i(r) = \phi_i^2(r) = \sum_{\lambda=1}^{N} C_{i\lambda}^2(r) \quad (5)$$

In this way, a molecular orbital confined on a nucleobase displays an electron density equal to 1 and hence a maximal length for the line showing the electronic level on that site.[29]

III. Results and Discussion

The chemical structures of the DNA hairpins investigated in this work are shown in Figure 1. Because our focus here is on the distance dependence of the electronic matrix elements, V_{DA}, for photoinduced hole transfer from the chromophore to the guanine and how it is impacted by the nature of the donor, no attempt to model the thermodynamic aspects of the hole transfer has been made. Our analysis thus resides on the premise that β in eq 1 is mostly controlled by the electronic coupling, neglecting the role of the reorganization energy and of differences in Gibbs free energy.[30] This appears to be reasonable because assuming no (or a weak) distance dependence for the activation energy is consistent with the very similar values of falloff parameter measured experimentally for the electronic coupling V_{DA} and the transfer rate k_{DA} in DNA hairpins linked with the SA chromophore; it should be borne in mind that the V_{DA} falloff was deduced from a fit of the driving force dependence of the charge-transfer rates using a Marcus/Jortner-like second-order expression (where k_{DA} is proportional to V_{DA}^2)

(24) Cornell, W. D.; Cieplak, P.; Bayly, C. I.; Gould, I. R., Jr.; Merz, K. M.; Caldwell, J. W.; Kollman, P. A. *J. Am. Chem. Soc.* **1995**, *117*, 5179.
(25) Dewar, M. J. S.; Zoebisch, E. G.; Healy, E. F.; Stewart, J. J. P. *J. Am. Chem. Soc.* **1985**, *107*, 3902.
(26) Dewar, M. J. S.; Ampac 6.55 ed.; Semichem: 7204 Mullen, Shawnee, KS 66216, 1997.
(27) Lewis, F. D.; Liu, X.; Wu, Y.; Miller, S. E.; Wasielewski, M. R.; Letsinger, R. L.; Sanishvili, R.; Joachimiak, A.; Tereshko, V.; Egli, M. *J. Am. Chem. Soc.* **1999**, *121*, 9905.
(28) Sugiyama, H.; Saito, I. *J. Am. Chem. Soc.* **1996**, *118*, 7063.
(29) Within the McConnell picture, the basis functions are totally localized, so that each of the ρ_i would be either unity or zero. The departures of the actual line representations in Figure 3 from this picture graphically show the delocalization, described in the McConnell treatment by perturbation theory.
(30) Tavernier, H. L.; Fayer, M. D. *J. Phys. Chem. B* **2000**, *104*, 11541.

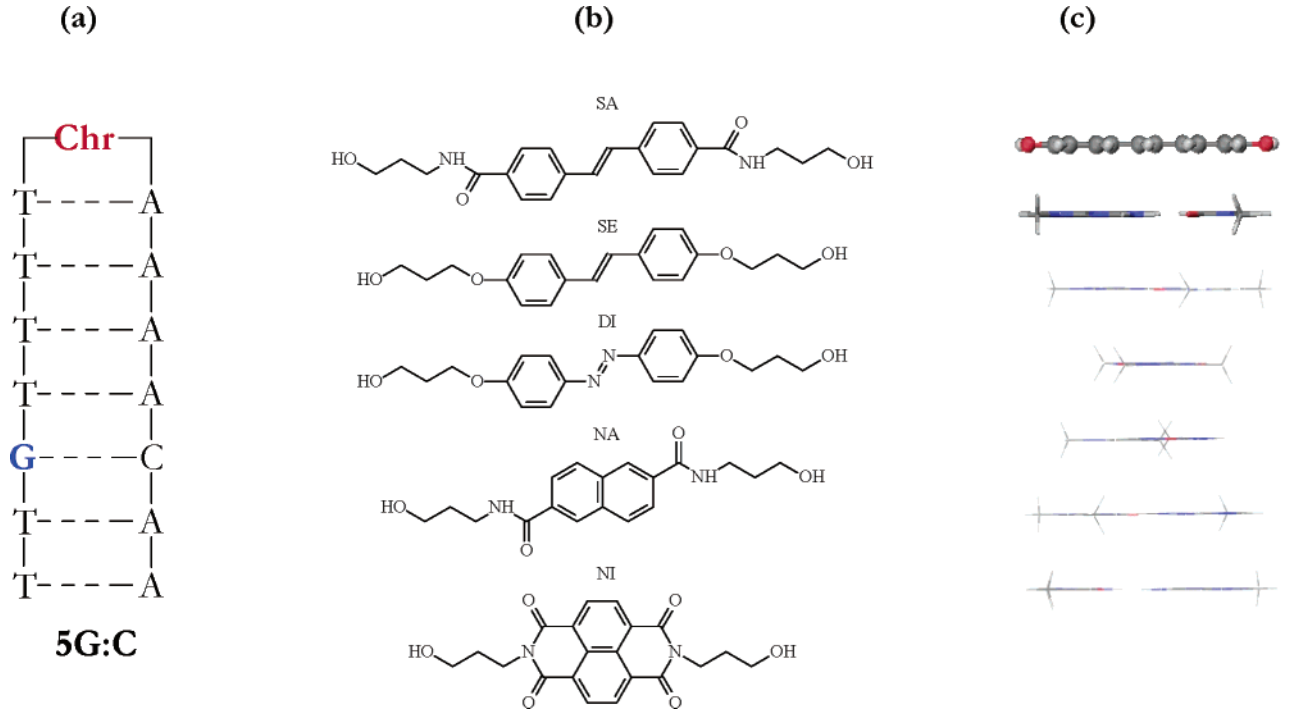

Figure 1. (a) Chemical structure of DNA hairpins. Chr denotes the chromophore, which in the actual structures is covalently linked to the DNA backbone through the end-groups. The position of the guanine is varied along the stack, from position 1 to position 5; (b) chemical structures of the chromophores investigated; (c) side view of the SE-GAAAAAA constrained model hairpin.

Table 1. Comparison between the Measured[18] and INDO/SCI-Calculated Vertical Transition Energies from the Relaxed Lowest Optically Allowed Excited State to the Ground State of the Isolated Chromophores

	INDO/SCI (eV)	exp. (eV)
SA	3.38	3.35
SE	3.43	3.45
NA	3.49	3.55
NI	3.50	3.24

in a series of hairpins with different hole donor and acceptor units.[18] We further note that very high values (on the order of 10^2) have recently been reported for the (poorly defined) effective internal longitudinal dielectric constant of DNA, possibly as a result of the solvation of the terminal phosphate groups;[31] the Coulombic interactions between the opposite charges carried by the donor and acceptor sites in the charge-separated state are thus expected to be strongly screened, leading to a weak dependence of the energetics on donor−acceptor separation.

Photoinduced electron-transfer reactions are initiated upon excitation of the chromophore by a vertical electronic transition from the ground state to the excited state, followed by nuclear relaxation on the excited potential energy surface toward the D*A equilibrium geometry. A proper description of the electronic structure in the chromophore excited state is therefore of crucial importance to quantify the electronic couplings for the charge-transfer process. We have calculated these values assuming that the donor relaxes internally before charge transfer. Excellent agreement is found between the calculated and measured chromophore emission energies, see Table 1, which again validates the choice of the INDO/SCI technique; these energies are within a few hundredths of an electronvolt of the experimental values of Lewis et al.[18] except for NI (where the difference is 0.26 eV).

(31) Williams, T. T.; Barton, J. K. *J. Am. Chem. Soc.* **2002**, *124*, 1840.

Table 2. Electronic Couplings (V_{DA} in cm^{-1}), Transition Moments (μ_{RP} in Debye), State Dipole Differences ($\Delta\mu_{RP}$ in Debye), and Energy Offsets (ΔE_{RP} in eV) Involved in the Generalized Mulliken−Hush Formalism for Charge Transfer (Eq 1), as a Function of the Distance d (in Å) between the Chromophore (Donor) and the Guanine (Acceptor)

	SE				NI			
d	V_{DA}	μ_{RP}	$\Delta\mu_{RP}$	ΔE_{RP}	V_{DA}	μ_{RP}	$\Delta\mu_{RP}$	ΔE_{RP}
3.2	292	1.41	12.1	0.32	−2375	3.92	15.7	−1.32
6.6	36.7	0.10	22.3	1.00	−369	1.36	29.6	−1.36
10.0	32.5	0.12	40.9	1.37	−9.9	0.08	47.3	−0.69
13.4	18.8	0.09	61.4	1.66	−1.0	0.02	63.3	−0.43
16.8	12.3	0.06	77.2	1.88	−1.9	0.08	78.1	−0.22

	SA				NA			
d	V_{DA}	μ_{RP}	$\Delta\mu_{RP}$	ΔE_{RP}	V_{DA}	μ_{RP}	$\Delta\mu_{RP}$	ΔE_{RP}
3.2	−158	2.29	16.1	−0.14	1293	7.05	3.79	0.33
6.6	25.4	0.32	33.0	0.32	61.9	0.39	27.8	0.54
10.0	1.6	0.02	49.5	0.58	15.9	0.07	39.0	1.11
13.4	3.1	0.03	64.7	0.80	9.6	0.07	61.7	1.11
16.8	1.6	0.01	80.6	1.60	2.0	0.01	76.0	1.39

On the basis of the INDO/SCI description of the relaxed hairpin excited states, the electronic tunneling matrix elements for photoinduced hole transfer were calculated using the GMH approach. Table 2 lists the electronic couplings (V_{DA}), transition moments (μ_{RP}), state dipole differences ($\Delta\mu_{RP}$), and energy differences (ΔE_{RP}) computed for the systems investigated in this work. As expected for a tunneling process, $\ln(V_{DA}^2)$ follows more or less a linear evolution with donor−acceptor distance, as shown for two representative sets of molecules (SE and NA hairpins, leading to a slow and fast decay of the transfer rate with donor−acceptor separation, respectively) in Figure 2; the slopes obtained through a linear regression of the squared

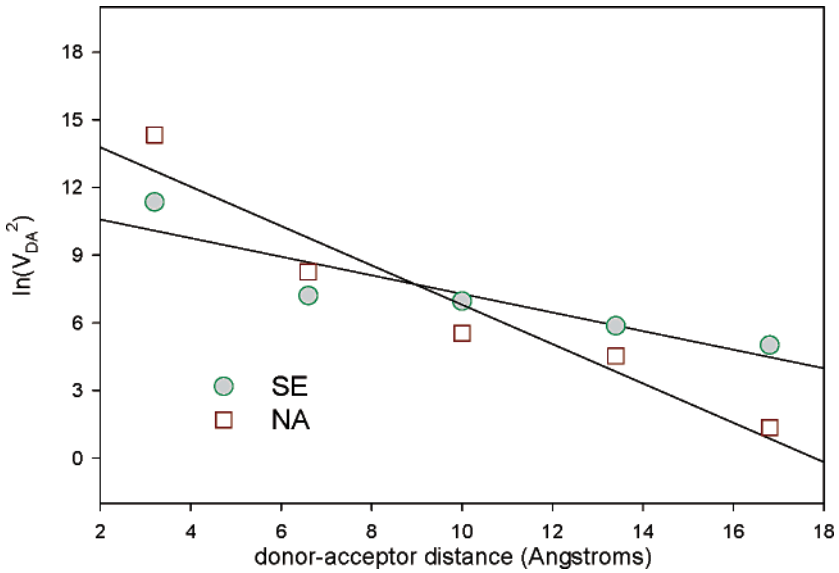

Figure 2. Distance dependence of V_{DA} for the NA and SE linkers.

Table 3. Falloff Parameters, β, Obtained by a Linear Fit of the V_{DA} Values Calculated for the Different Chromophores[a]

	β (Å^{-1})
NI	1.18 (1.06)
NA	0.87 (0.64)
SA	0.66 (0.45)
SE	0.41 (0.23)

[a] The values in parentheses have been obtained by removing the first point (with donor and acceptor in direct contact) in the fit, see text.

electronic couplings, that is, the falloff parameters β, are collected for the different hairpins in Table 3. Note that the first point in the different series investigated corresponds to the situation where the chromophore hole donor is in direct contact with the guanine hole acceptor. Because, as mentioned above, it is not clear that in this case the perturbation theory used to describe the through-bridge hole migration, which leads to eq 1, is applicable, we have also listed in Table 3 the β values obtained by removing the first point in the linear regressions.

The β value calculated for SA, 0.66 Å^{-1} [0.45 Å^{-1} when ignoring the first point], is in good agreement with the experimental one, 0.58 Å^{-1},[18] which confirms the reliability of the present theoretical approach (in particular, it suggests that most of the distance dependence of the transfer rate is dominated by the electronic factor V_{DA}). Most importantly, the β values show significant dispersion: they vary from ~0.4 [0.23, when the first point is removed] Å^{-1} in SE end-capped sequences to ~1.1 Å^{-1} in hairpins possessing a NI linker. Thus, the nature of the donor has a significant influence on the distance dependence of the photoinduced hole transfer to guanine. This feature can be rationalized on the basis of the description of the main channels involved in the charge-separation mechanism and follows from the simple McConnell model where V_{DA} across an n-unit bridge is expressed in terms of the coupling between the donor and the bridge (T_D) and the energy gap between the chromophore and the bridge subunit (Δ), as well as in terms of the hopping integral along the bridge (t) and the acceptor−bridge coupling (T_A):[32,33]

$$V_{DA} \cong (T_D T_A/\Delta)(t/\Delta)^{n-1} \quad (6)$$

In all cases, we find that the transition moment between the initial and final adiabatic states, μ_{RP}, dominates the evolution with distance of the tunneling matrix element. This is reasonable because none of the other factors in eq 2 should be strongly distance dependent. From a detailed analysis of the main contributions to μ_{RP}, two major aspects can be underlined: (i) the importance of the energy mismatch between the electronic levels of the chromophore and the intervening AT base pairs, that is, the injection barrier;[19] and (ii) the importance of the overlap between the corresponding wave functions, which depends critically on symmetry and spatial confinement. Note that these two aspects are related to Δ and T_D in McConnell's expression, respectively. Both effects can be analyzed from the hairpin one-electron energy diagrams, using the graphical representation for the molecular orbital spatial delocalization described in the methodology section. These diagrams are shown in Figure 3 for representative hairpins linked with the NI, SA, and SE chromophores.

For all hairpins investigated, the highest occupied molecular orbital (HOMO) of the ground-state structure is localized on the guanine site (with the lowest ionization potential); the adenines lead to the formation of a set ("band") of molecular orbitals located below the guanine HOMO (G_H) and slightly delocalized through the DNA bridge (as do thymines but at still lower energy). Especially, we can identify two such bands, centered around ~ −7.0 eV (A_H band) and ~ −8.0 eV (A_{H-1}

(32) McConnell, H. M. *J. Chem. Phys.* **1961**, *35*, 508.
(33) Ratner, M. A. *J. Phys. Chem.* **1990**, *94*, 4877. Skourtis, S. S.; Onuchic, J. N.; Beratan, D. M. *Inorg. Chim. Acta* **1996**, *243*, 167.

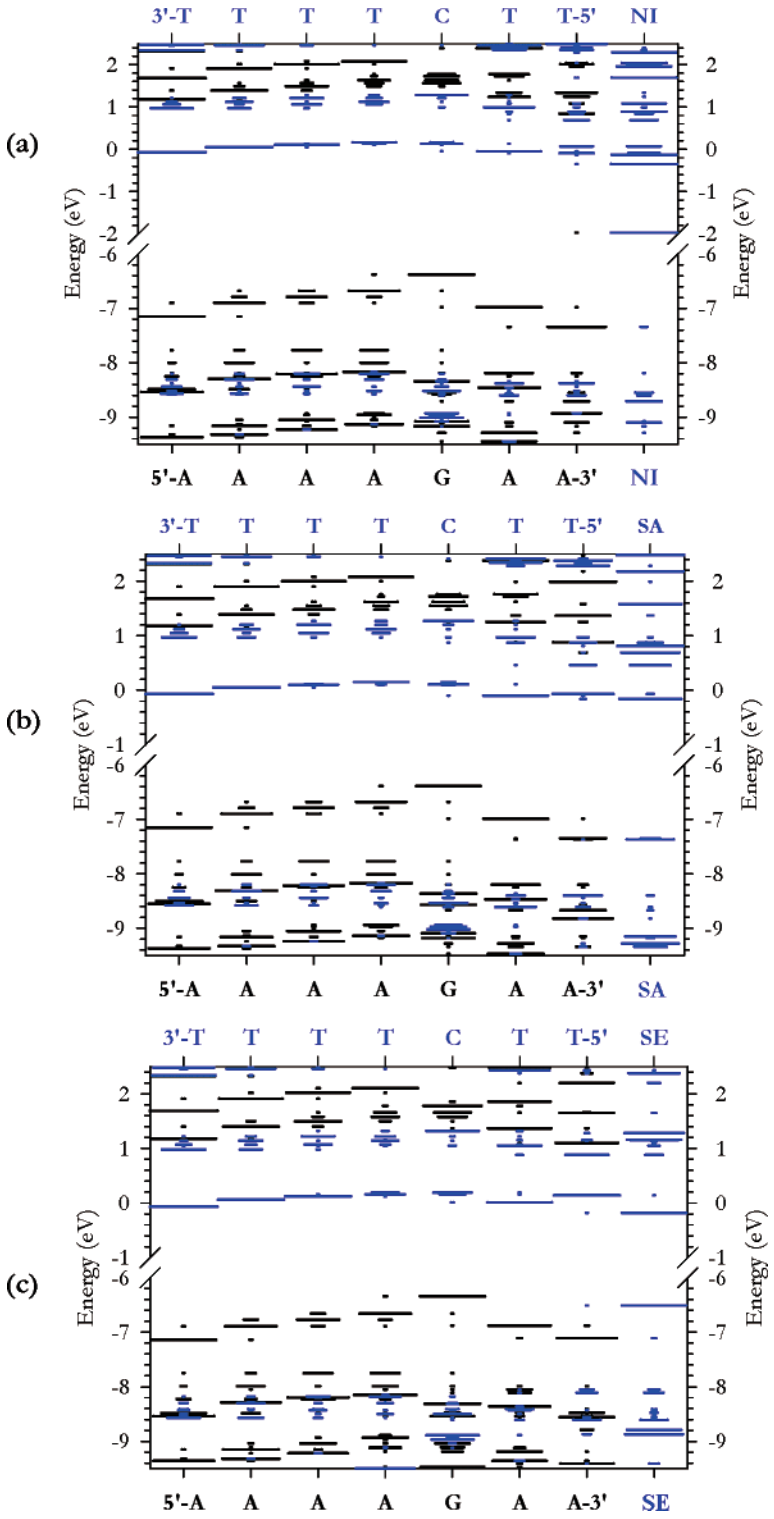

Figure 3. Electronic structure of the NI (a), SA (b), and SE (c) hairpins. Each molecular orbital is depicted on the basis of one or several horizontal lines, whose width per base is proportional to the site electron population, see methodology. Note that two colors have been used to differentiate the contributions from bases belonging to the complementary strands.

band) at the INDO level, Figure 3. Note that the A_{H-1} band has a more delocalized character than A_H due to a more efficient wave function overlap.

Because of the presence of the strong electron-withdrawing imide groups, NI has a much larger ionization potential than G or A. Therefore, the gap Δ for charge injection is high, preventing any significant mixing between the NI HOMO level and the A_H band of the intervening adenine bases (the major contributions to the transition moment and hence electronic coupling in fact come from configurations involving low-lying thymine- and adenine-based molecular orbitals with small contributions to the excited-state wave functions, eq 3); this leads to a high β value (1.06−1.18 $Å^{-1}$).

Along the same line, β is significantly reduced when going from NI to SA, for which there is an almost perfect match between the HOMO of the chromophore and the HOMO band

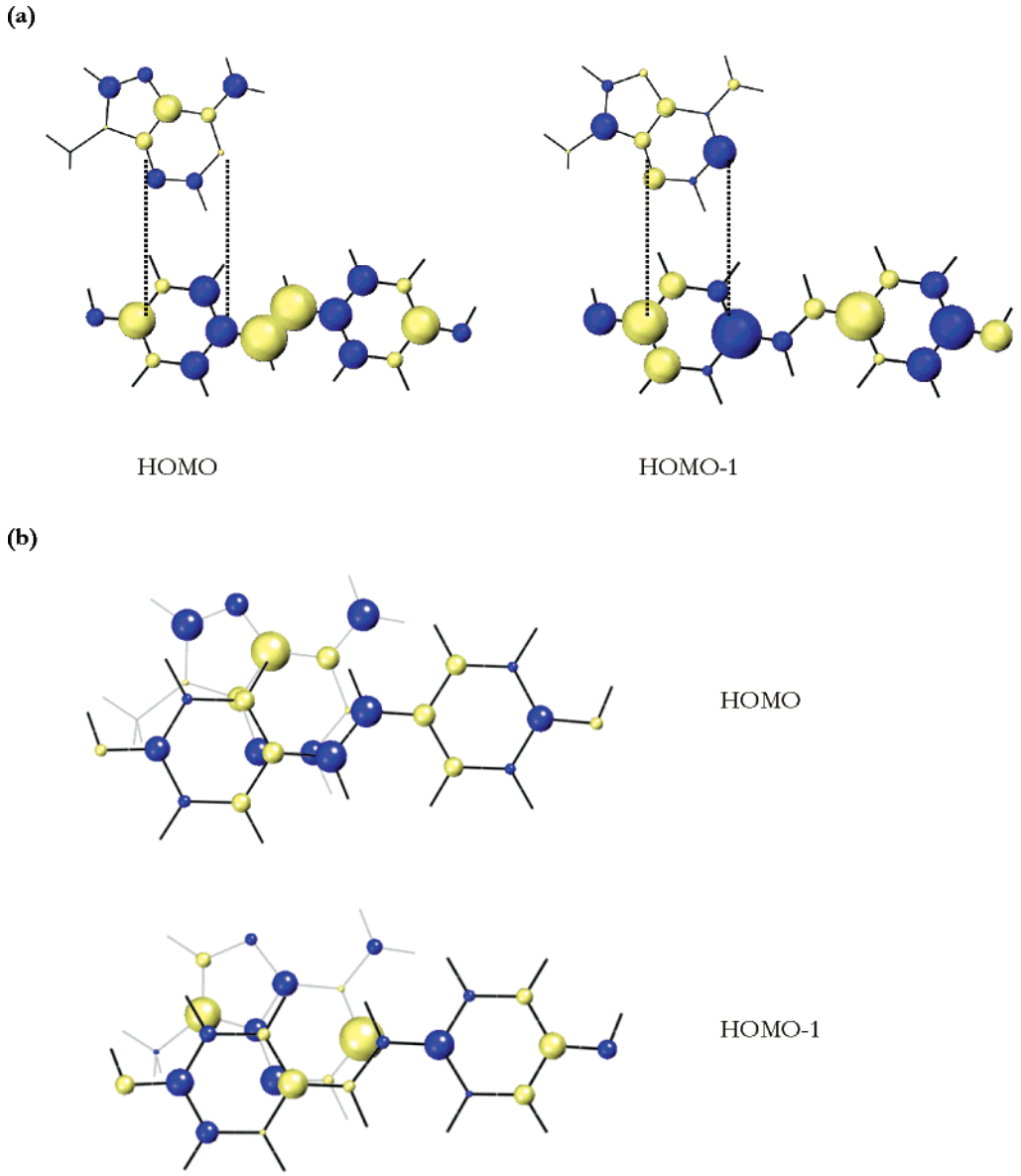

Figure 4. Schematic representation of the isolated SE chromophore and adenine HOMO and HOMO−1 molecular orbitals. (a) Cofacial packing of the molecules. (b) Actual packing in the hairpins. Note that the SA MOs are similar to those of SE.

formed by the bridge adenine bases, that is, A_H (Figure 3). However, in contrast to what is expected on the basis of Hückel-type calculations[19] (and despite the fact that the chromophore excited-state wave function is dominated by configurations involving the SA HOMO level), bandlike transport with the charge completely spread out over the bridge is not observed; the main rationale for our result is the limited overlap between the involved orbitals, which can be understood on the basis of symmetry considerations: the SA and adenine HOMOs (Figure 4) display an antibonding overlap pattern that prevents delocalization within the SA/hairpins. This can be clearly inferred from the shape of the HOMO orbitals in the isolated SA and adenine molecules when assuming a cofacial arrangement of the benzene rings (Figure 4a, left); the actual packing of the molecules in the hairpins is, however, slightly different (Figure 4b, top) and allows for some coupling, albeit weak, between the chromophore and the adjacent adenine base.

Strikingly, even though its HOMO level lies significantly above that of adenine (which is a result of the destabilizing effects induced by the electron-donating alkoxy groups), SE leads to the weakest dependence on donor−acceptor separation ($\beta \approx 0.4$ or 0.23 Å^{-1}, depending on whether the first sequence is included in the fit or not). It turns out that, in this molecule, the HOMO−1 molecular orbital has the appropriate symmetry (and energy) to interact with the HOMO−1 band of the poly(AT) sequence, that is, A_{H-1} (Figure 4a, right, and Figure 4b, bottom). This opens up a new pathway for charge migration (where the relevant orbitals in the expansion of μ_{RP} in eq 3 correspond to the SE and adenine HOMO−1 molecular orbitals), which is characterized by a significant amount of electron density delocalization over the bridge; an example of such a delocalized molecular orbital is shown in Figure 5. Similar conclusions can be drawn from the analysis of other donor-substituted stilbene linkers, where the contributions of the different channels to the overall electronic coupling result from a subtle interplay between the relative locations and shape of the involved molecular orbitals and their contributions to the D*A and D^-A^+ excited states description.

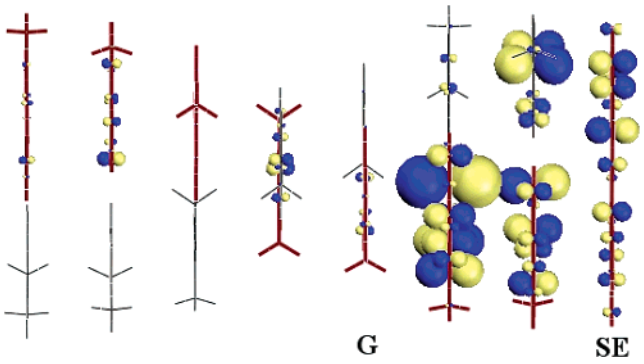

Figure 5. A delocalized molecular orbital of the SE-AAGAAAA model hairpin, resulting from the interaction between the HOMO−1 level of the chromophore and the A_{H-1} band (formed by the overlap of the adenine HOMO−1 orbitals).

IV. Conclusions

We have shown that the efficiency for hole injection into DNA hairpins results from the interplay between two key factors: the electronic mismatch between the donor and the bridge electronic levels and the coupling between the corresponding orbitals. In stilbene chromophores bearing electron-donating groups, a new channel for charge migration involving the close-lying HOMO−1 orbitals of the donor and the poly(AT) sequence has been identified; this channel can promote long-distance hole transfer.

This work clearly shows that the conductance properties of DNA hairpins cannot be unambiguously estimated only on the basis of the measured injection energy, but that the impact of donor-bridge overlap must also be taken into account.[33] For this purpose, quantum-chemical calculations performed on the actual molecular structures and allowing for multiple charge-transfer pathways prove to be useful.

It would be most interesting to try and generalize the results obtained here for model DNA hairpins to the individual charge-hopping steps in double-strand DNA where an oxidized guanine site plays the role of the hairpin excited chromophore. We stress that structural fluctuations effects and a more complete account of the medium should be considered for a detailed description of the dynamics of photoinduced charge generation in DNA. However, we believe that the relationships between the chemical nature of the linker chromophore and hole-transfer falloff parameter that have been identified in the present work will remain applicable when taking into account these effects in a more sophisticated approach.

Acknowledgment. The work at Georgia Tech is partly supported by the National Science Foundation (awards CHE-0078819 and CHE-0342321) and the IBM Shared University Research Program. The work in Mons is partly supported by the Belgian Federal Services for Scientific, Technical, and Cultural Affairs (InterUniversity Attraction Pole 5/3) and the Belgian National Science Foundation (FNRS). D.B. is an FNRS Senior Research Associate. Work in Evanston is supported by the DoD MURI program.

JA035596F